Identifying the Distinct Phases of Carrier Transport in Semiconductors with 10 fs Resolution

B. B. Hu, E. A. de Souza, W. H. Knox, J. E. Cunningham, and M. C. Nuss
AT&T Bell Laboratories, 101 Crawfords Corner Road, Holmdel, New Jersey 07733-3030

A. V. Kuznetsov
Department of Physics, University of Florida at Gainesville, Gainesville, Florida 32611

S. L. Chuang
Department of Electrical and Computer Engineering, University of Illinois at Urbana-Champaign, Urbana, Illinois 61801-2991
(Received 24 October 1994)

We study the very early processes of photogenerated carrier transport in GaAs and Si using THz nonlinear spectroscopy with 10 fs time resolution. This ultrahigh time resolution allows us to clearly separate the instantaneous creation of polarized electron-hole pairs and the subsequent carrier motion for the first time. In addition, our results give the first clear demonstration of the distinct phases of carrier transport; ballistic transport, electron velocity overshoot, and steady-state drift.

PACS numbers: 78.47.+p, 42.65.Re, 72.15.Lh, 84.40.Cb

When a semiconductor structure is excited by a light pulse, electron-hole pairs are created with some excess energy. Under a bias field, they move in a complex manner, depending on the material band structure, electric field, and the geometry. The carrier transport process is further complicated by events such as carrier-phonon interaction, carrier-carrier scattering, intervalley scattering, and impurity scattering. Carrier transport dynamics are relevant in the operation of high-speed electronic and optoelectronic devices such as transistors, photodetectors, and modulators. Many studies of these transport processes have been performed to date [1–3]. In the present case, we consider only the very first events in carrier transport. In order of time scale, the carrier transport process can be divided into four different stages. In the first stage, when a biased semiconductor is excited by an ultrashort light pulse, an instantaneous polarization of the photoinjected electron and hole pairs is created [4,5]. In the second stage, carriers undergo ballistic acceleration without scattering by the electric field for times shorter than the mean scattering time ($\sim 10^{-13}$ s). In the third stage, as carrier-carrier and carrier-phonon scattering processes set in, the acceleration of the carriers stops, and the average drift velocity reaches a maximum. Velocity overshoot occurs for materials such as GaAs, when hot electrons are scattered into satellite L, X valleys with lower mobility. In the fourth stage, the velocity is maintained at a lower level in steady-state drift. These four time regimes, while easily defined, have not been clearly separated to date because scattering times limit the ballistic regime to ~50 fs for typical conditions. The instantaneous polarization has been discussed previously [4–6]; however, it has only been isolated in THz emission from a multiple quantum well (MQW) structure where carrier transport is inhibited [7,8]. In bulk samples, the lack of time resolution in previous experiments has hampered the clear distinction of both the instantaneous polarization and the ballistic transport of the photocarriers in the time domain, although some evidence for ballistic transport was reported [9]. Although, experimentally, the overshoot feature in the transient photocurrent was investigated by several groups using different techniques such as electroabsorption, electro-optic sampling, and photoconductive sampling [10–12], many uncertainties still remain since space-charge effects were shown to produce a similar overshoot feature [13].

Here, we present a study of the field screening after injection of electron-hole pairs by using THz spectroscopy with 10 fs resolution. Be detecting the change of the dc field, we clearly separate the instantaneous polarization and carrier transport in the time domain. In addition, we show directly that in the first roughly 70 fs the electrons and holes are accelerated ballistically, and that the average drift distance increases quadratically in time. At later times, we observe that the electron drift velocity reaches a maximum value, and then relaxes down to a steady-state value. The time it takes for the drift velocity to overshoot its steady-state value is roughly 200 fs. This time is about a factor of 2 shorter than the theoretically predicted value [14], suggesting that further examination of transport models will be necessary. To our knowledge, these are the first unambiguous observations of the initial events in carrier transport. It is worth pointing out that, because our excitation spectrum excites e-h pairs mostly above the band gap into continuum states, Coulomb interactions are small and are not likely to influence our results. It has also been shown that, unlike the optical interband polarization, the *intraband* e-h polarization measured here is not very sensitive to many-body interactions [8], so that we can expect our experiments to be a good measurement of free-carrier transport phenomena.

Our experimental technique is to inject electron-hole pairs with a 10 fs optical pulse into the field region of a large-aperture GaAs Schottky diode. When the change of the field by the photocarriers is small, it can

 © 1995 The American Physical Society

be approximated by $\Delta E_{dc}(t) = -[P_{instan}(t) + Nex(t)]/\varepsilon$, where $P_{instan}(t)$ is the instantaneous e-h polarization, N is the photocarrier density, $x(t)$ the average displacement between electrons and holes at time t after the excitation, ε the dielectric constant, and e the electron charge. This change of the field is probed by detecting the THz signal from the second time-delayed optical pulse. The total THz energy is proportional to the square of the bias field, so that the relative change of the THz energy is given by

$$\frac{\Delta W(t)}{W} = \frac{2\Delta E_{dc}(t)}{E_{dc}} = -\frac{2}{E_{dc}\varepsilon}[P_{instan}(t) + Nex(t)], \quad (1)$$

where $\Delta W(t)$ is the change of THz energy from the second pulse at time t after the prepulse, W is the total THz pulse energy, and E_{dc} is the unscreened bias field. Hence, by monitoring the change in THz energy as a function of time, we directly map out the transport movement of the carriers generated by the prepulse. We would like to point out that, although the optical absorption depth is on the order of the GaAs layer thickness, the measured signal only depends on the total number of e-h pairs excited and not on their spatial distribution as long as the space-charge field is small compared to the applied field. The time resolution in this technique is limited only by the optical pulse duration. Since the speed of the instantaneous polarization is determined by the laser pulse duration, while the speed of the transport component $Nex(t)$ is limited by the reduced effective mass of the electron-hole pairs and the electric field, we can clearly separate the instantaneous polarization and carrier transport in time. Furthermore, since we directly trace the movement of the photocarriers in time with 10 fs resolution, we are able to obtain the exact time dependence of the average drift distance and hence the velocity. It is worth emphasizing that this is a nonlinear THz technique, and we measure directly the displacement of electrons and holes, rather than the photocurrent as in previous experiments. Also, the interpretation of our results is not complicated by space-charge effects [14]. In fact, in our experiments, the space charge *is* the probe of carrier movement.

Both a bulk GaAs sample and a MQW sample are used in our experiments. These samples are metal-i-n Schottky diodes grown by a molecular beam epitaxy. For the bulk sample, the intrinsic region consists of a 1.7 μm GaAs layer sandwiched by 3500 Å $Al_{0.5}Ga_{0.5}As$ layers. The sample is capped with 100 Å GaAs, and finally, a 50 Å Ti film is deposited. A large and uniform electric field in the intrinsic region can be achieved by applying a reverse bias voltage between the semitransparent metal film and the heavily doped substrate. The THz signal measured from this sample increases linearly with the reverse bias and vanishes at flat band (1.2 V). The MQW sample is similar to the bulk sample with the 1.7 μm GaAs layer replaced by 100 periods of $GaAs/Al_{0.32}Ga_{0.68}As$ (120 Å/150 Å). For comparison, we also design a Si p-i-n diode for the experiment. It has a n^+-doped top layer of 500 Å, an intrinsic region of 7 μm, on a p^+ substrate.

Figures 1(a), 1(b), and 1(c) show the laser spectrum, GaAs absorption spectrum, and the schematic experimental setup, respectively. The optical source is a self-focusing-mode-locked Ti:sapphire laser pumped by a cw argon ion laser [15]. It produces optical pulses with a duration of 10 fs at a repetition rate of 82 MHz. The laser beam is delivered into a Michelson interferometer. One arm of the Michelson is mounted on a piezoelectric transducer (PZT) controlled stage, while the other arm is on a translation stage, so that the relative time delay and optical phases of the two pulses can be adjusted. The pair of pulses from the Michelson interferometer is weakly focused and strikes the sample at an incident angle of 60°, resulting in a carrier density of roughly 10^{15} cm^{-3} for a beam size of 0.5×0.5 mm^2 on the sample. One pulse (pulse 2) is chopped, so that only the THz signal generated by pulse 2 is detected, while pulse 1 merely injects carriers into the semiconductor. The THz signal is collected by a pair of off-axis paraboloids (not shown in Fig. 1) and detected by a 50 μm photoconductive dipole antenna with a silicon hyperhemispherical substrate lens attached [16]. The THz energy $W(t)$ is computed by squaring and time integrating each THz wave form. In order to eliminate optical interference fringes, we scramble the optical phase of pulse 1 by shaking one of the Michelson mirrors using the PZT with an amplitude of about a single wavelength.

Figure 2 shows results from the three samples. The solid lines are numerical fits to the experimental curves. The left vertical axis is the field-normalized change in THz energy $(\Delta W/W)E_{dc}$ from the second pulse, while the right vertical axis shows the average displacement in angstroms for the bulk GaAs sample using Eq. (1). For reference, we also plot the second harmonic autocorrelation of the optical

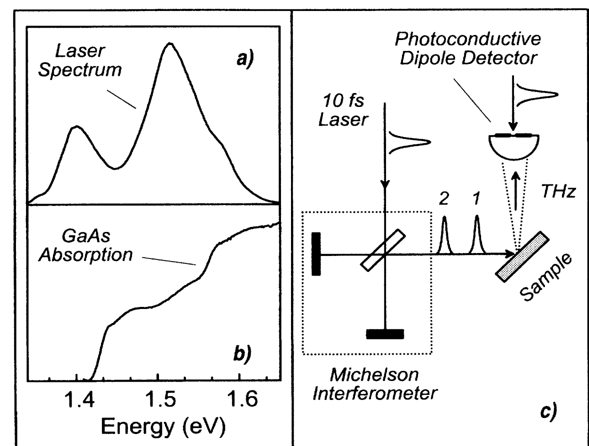

FIG. 1. (a) The spectrum of the 10 fs laser pulse. (b) The GaAs absorption spectrum. (c) Schematic of the experimental setup.

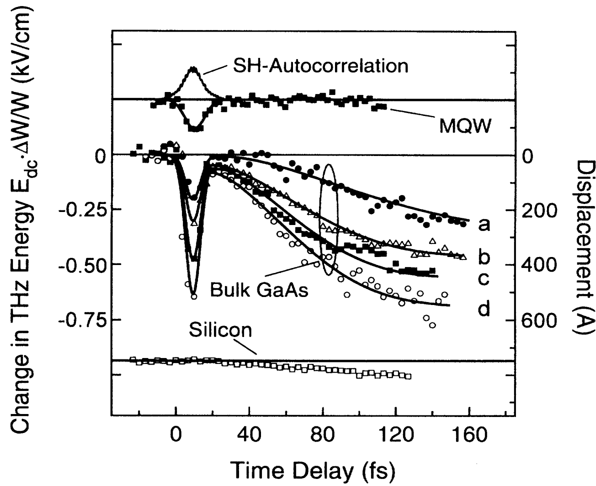

FIG. 2. The measured THz energy as a function of time delay relative to the prepulse for three samples: bulk GaAs, GaAs-MQW, and silicon. The bias field for curves *a*, *b*, *c*, and *d* are 15.8, 17.8, 20, and 23 kV/cm, respectively. The bias field in the intrinsic region of the Si *p-i-n* diode is roughly 50 kV/cm. The builtin field of the MQW sample is 20 kV/cm. The solid curves are numerical fits to the experimental data. For reference, the intensity autocorrelation trace of the optical pulse is also plotted.

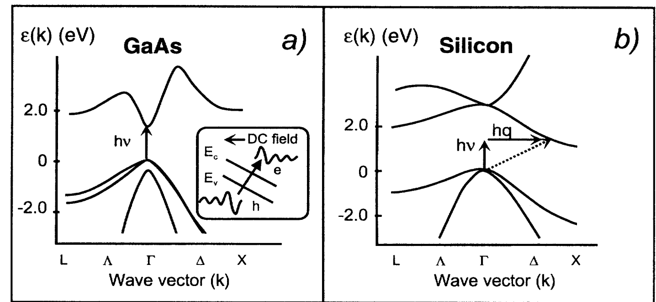

FIG. 3. (a) The schematic band diagram for GaAs. Inset shows the spatially nonvertical transition responsible for the instantaneous electron-hole polarization. (b) The band diagram for Si.

pulse. For the MQW sample, we observe a fast dip with a width comparable to the pulse duration. For the bulk GaAs sample, in addition to the fast dip, we observe a slower decay in THz energy. Both the amplitude of the fast dip and the decay increase with the bias field. In contrast, in the silicon *p-i-n* sample, we only observe a decay without the initial dip. We also repeat the measurement for GaAs at different crystal orientations by rotating its azimuth angle (not shown). No crystal orientation dependence is observed, indicating that the bulk $\chi^{(2)}$ effect is negligible in our experiments [17,18].

The fast dip observed in the MQW and GaAs samples is clearly the instantaneous electron-hole polarization, since it is the only contribution to the THz signal in the MQW sample [7], while in the bulk sample the carriers can hardly move any distance during the first 10 fs. The instantaneous polarization is a macroscopic dipole moment generated by directly exciting the electrons and holes into states which are polarized by the dc electric field [see Fig. 3(a)] [4,5]. It arises from the coherence of the electron and hole wave functions. For an indirect band gap material such as Si, optical creation of an electron-hole pair is achieved through incoherent random optical phonon scattering which destroys the coherence between the electrons and holes [Fig. 3(b)]. As a result, we do not observe the instantaneous polarization in the silicon sample (lower trace in Fig. 2).

The instantaneous polarization consists of a resonant contribution which follows the time integral of the optical pulse, and an off-resonant contribution which follows the optical pulse envelope. In a bulk or a MQW sample when continuum states are excited, it is estimated that the off-resonant contribution dominates and the overall instantaneous polarization follows the optical pulse envelope [5]. This polarization sets up a space-charge field which reduces the existing field, and thus also diminishes the THz signal. When the two pulses overlap in time, the dip in THz signal is detected due to the cross correlation between the instantaneous polarizations from each pulse. In our experiments, the width of the dip is comparable to the optical pulse duration, showing that the speed of the polarization of electron-hole pairs is limited only by the optical pulse.

The subsequent increase of the electron-hole displacement in the bulk GaAs and silicon samples represents the field screening due to the space-charge field set up by electrons and holes as they separate. At early times, we expect that the carriers are accelerated ballistically in the electric field. This is illustrated in Fig. 2 as the average displacement in the first 70 fs can be fitted by a quadratic time dependence. This is the first clear time-domain observation of ballistic transport in a semiconductor. By fitting the experimental curves with $eE_{\mathrm{dc}}t^2/2m^*$, we obtain an average reduced effective mass m^* of $0.043m_0$ for fields at 23, 20, and 17.8 kV/cm, where m_0 is the electron mass. This number is close to the literature value. The literature value of the reduced mass is $0.056m_0$ for electrons and heavy holes, and $0.034m_0$ for electrons and light holes, with a population ratio for heavy holes and light holes of roughly 2:1.

At times >70 fs, the displacement deviates from the quadratic time dependence as scattering processes set in. The major scattering processes which can affect the drift velocity on this time scale are electron-hole scattering, electron-LO-phonon scattering, and electron and intervalley phonon scattering. In our measurements, the carrier density is about 10^{15} cm^{-3}, and electron-hole scattering is negligible. Also, electron-LO-phonon scattering time is measured to be 170 fs [19]. Our observation of ballistic transport only within the first 70 fs suggests that the

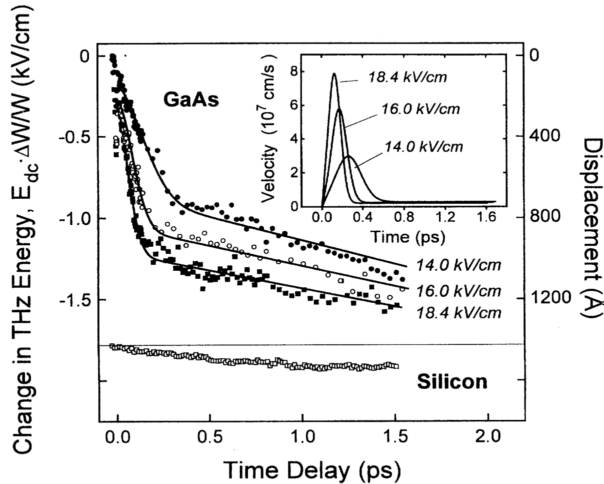

FIG. 4. The measured THz energy as a function of time for bulk GaAs on a longer time scale. The solid curves are numerical fits to the experimental data. Inset: The time derivative of the numerical fits to the data. The bottom curve shows the results for the Si sample.

electron-intervalley scattering takes place rapidly as the electrons are ballistically accelerated by the field.

Figure 4 shows the results from the bulk GaAs sample and the Si *p-i-n* sample on a longer time scale. The solid lines are numerical fits to the experimental data. For the GaAs sample, the displacement increases rapidly within the first 200 fs, then linearly in time at a much slower rate. In contrast, for the Si sample, the displacement always increases linearly with time. The different slopes observed at different times in the GaAs sample directly reflect transient velocity overshoot. By taking the time derivative of the solid lines, we can obtain the time dependence of the relative electron-hole drift velocity as shown in the inset of Fig. 4. The overshoot feature is very prominent. For a field of 18.4 kV/cm, we observe that the drift velocity reaches its maximum overshoot value in about 100 fs, and then relaxes down to its steady-state value in about 200 fs. The time scale we observed here is much shorter than that from previous Monte Carlo simulations [14]. Also, the amount of the overshoot observed is roughly twice as large as theoretically estimated. This discrepancy between our results and previous Monte Carlo simulations warrants a critical examination of our understanding of current transport on a 10 fs time scale.

In summary, for the first time, we clearly separate the instantaneous polarization from carrier transport occurring on a time scale of less than 100 fs. We confirm that the instantaneous polarization is as fast as the optical pulse. Furthermore, we directly trace the transport motion of electrons and holes in different electric field with 10 fs resolution. We show that electron and holes are ballistically accelerated by the field within the first 70 fs. At later times, we observe that the drift velocity overshoots its steady-state value in roughly 200 fs. Our experiments thus clearly reveal the distinct stages in the photoconductive response of the semiconductors.

We would like to acknowledge valuable discussions on electron velocity overshoot with Steve Goodnick. We are also grateful to Ran Yan for providing the silicon *p-i-n* sample used in the experiments. S. L. C. is supported by ONR under Grant No. N00014-90-J-1821.

[1] L. Reggiani, *Hot-Electron Transport in Semiconductors,* Springer-Verlag Topics in Applied Physics Vol. 58, (Springer-Verlag, Berlin, 1984).
[2] J. Shah, *Hot Carriers in Semiconductor Nanostructures* (Academic Press, Inc., New York, 1992).
[3] M. C. Nuss D. H. Auston, and F. Cappasso, Phys. Rev. Lett. **58**, 2335 (1987).
[4] S. L. Chuang, S. Schmitt-Rink, B. I. Greene, P. N. Saeta, and A. F. J. Levi, Phys. Rev. Lett. **68**, 102 (1992).
[5] A. V. Kuznetsov and C. J. Stranton, Phys. Rev. B **48**, 10 828 (1993).
[6] B. B. Hu, A. S. Weling, D. H. Auston, A. V. Kuznetsov, and C. J. Stranton, Phys. Rev. B **49**, 2234 (1994).
[7] P. C. M. Planken, M. C. Nuss, W. H. Knox, D. A. B. Miller, and K. W. Goossen, Appl. Phys. Lett. **61**, 2009 (1992).
[8] M. C. Nuss, P. C. M. Planken, I. Brener, H. G. Roskos, M. S. Luo, and S. L. Chuang, Appl. Phys. B **58**, 249 (1994).
[9] W. Sha, J. K. Rhee, T. B. Norris, and W. J. Schaff, IEEE J. Quantum Electron. **28**, 2445 (1992).
[10] W. H. Knox, Appl. Phys. A **53**, 503 (1991).
[11] K. E. Meyer, M. Pessot, G. Mourou, R. Grodin, and S. Chamoun, Appl. Phys. Lett. **52**, 2148 (1988).
[12] C. V. Shank, R. L. Fork, and B. I. Greene, Appl. Phys. Lett. **38**, 104 (1981).
[13] A. E. Iverson, G. M. Wysin, D. L. Smith, and Antonio Redondo, Appl. Phys. Lett. **52**, 2148 (1988).
[14] G. M. Wysin, D. L. Smith, and A. Redondo, Phys. Rev. B **38**, 12 514 (1988).
[15] M. T. Asaki, C.-P. Huang, D. Garvey, J. Zhou, H. C. Kapteyn, and M. M. Murnane, Opt. Lett. **18**, 977 (1993).
[16] P. R. Smith, D. H. Auston, and M. C. Nuss, IEEE J. Quantum Electron. **QE-24**, 255 (1988).
[17] X. C. Zhang, Y. Jin, K. Yang, and L. J. Schowalter, Phys. Rev. Lett. **69**, 2303 (1992).
[18] B. I. Greene, P. N. Saeta, D. R. Dykaar, S. Schmitt-Rink, and S. L. Chuang, IEEE J. Quantum Electron. **QE-28**, 2302 (1992).
[19] J. A. Kash, J. C. Tsang, and J. M. Hvam, Phys. Rev. Lett. **54**, 2151 (1985).